International Journal of Scientific Engineering and Technology (ISSN : 2277-1581)
Volume No.3 Issue No.2, pp : 172 – 185 1 Feb 2014

Convective Heat and Mass Transfer Flow Over A Vertical Plate With Nth Order Chemical Reaction In A Porous Medium

Ime Jimmy Uwanta and Halima Usman
Department of Mathematics, Usmanu Danfodiyo University, Sokoto, Nigeria
Email: hhalimausman@yahoo.com

Abstract : The study of convective heat and mass transfer flow over a vertical plate with nth order chemical reaction in a porous medium is analyzed both analytically and numerically. The resulting governing boundary layer equations are highly non-linear and coupled form of partial differential equations and have been solved by using implicit finite difference method of Crank-Nicolson. To check the accuracy of the numerical solution, steady-state solutions for velocity, temperature and concentration profiles are obtained by using perturbation method. The effects of various parameters such as thermal Grashof number, solutal Grashof number, chemical reaction, order of chemical reaction, radiation, thermal conductivity, Prandtl number and Schmidt number on the velocity, temperature and concentration profiles as well as skin friction, Nusselt number and Sherwood number are presented graphically. The numerical results showed that both temperature and concentration increases with the increase in chemical reaction while velocity decreases. It was also observed that the numerical and analytical solutions are found to be in an excellent agreement.

Key words: heat and mass transfer, free-convection, porous medium and chemical reaction.

1. Introduction

The study of convective flow of heat and mass transfer with the influence of chemical reaction is given primary importance in science and engineering fields. This phenomenon plays an important role in chemical industry, hydro metallurgical industries, petroleum industry, cooling of nuclear reactors and packed –bed catalyst reactors Gregory and Ilhan [8].

Chemical reaction usually accompanies a large amount of endothermic and exothermic reactions. These characteristics could easily be seen in a lot of industrial processes. For example, in the power industry among the methods of generating electric power in which electrical energy is extracted directly from a moving conducting fluid. Recently, it has been realized that it is not always permissible to neglect the convection effects in porous constructed chemical reactors. The reaction produced in a porous medium was extraordinarily in common, such as in fuel cell modules and the polluted underground water because of the toxic substance Nield and Bejan [19].

In a recent literature review, porous media are widely used in high temperature heat exchangers, turbine blades, jet nozzles, solar collectors, drying processes, building constructions etc. In practice, cooling of porous structure is achieved by forcing the liquid or gas through capillaries of solid. Actually, they are used to insulate a heated body to maintain it is temperature. The effect of variable permeability on combined free and forced convection in porous media was analyzed by Chandrasekhar and Namboodiri [5]. Combined heat and mass transfer problems with chemical reaction are also important for a variety of engineering applications. These applications include solar collectors, grain storage and drying processes, heat exchangers, geothermal and oil recovery, building construction, nuclear waste material and many others Minto et al. [17]. In view of it is applications several authors have studied nth order chemical reaction and porous medium both in mechanical and physiological situations. Ahmad et al. [1] presented effect of first order chemical reaction and radiation on an unsteady MHD flow of an incompressible viscous electrically conducting fluid with variable temperature and mass transfer. Krishnendu [13] analyzed a steady boundary layer slip flow and mass transfer with nth order chemical reaction past a porous plate embedded in a porous medium. Also work on steady mixed convection flow in an incompressible viscous electrically conducting fluid with nth order chemical reaction has been reported by Gurminder et al. [9]. Additionally, a numerical investigation on the effect of chemical reaction on unsteady natural convection boundary layer flow over a semi-infinite vertical cylinder is carried out by Kawala and Odda [11].

A finite difference solution of the homogeneous first order chemical reaction on unsteady flow past an impulsively started semi-infinite vertical plate with variable temperature and mass transfer in the presence of thermal radiation have been examined

by Loganathan [14]. Mansour et al. [16] described the influence of chemical reaction and viscous dissipation on MHD natural convection flow. Recently, Dilal and Sewil [6] have studied a numerical model of the analysis of combined effects of mixed convection MHD heat and mass transfer in a visco-elastic fluid in a porous medium with chemical reaction, non uniform heat source/sink and visco-ohmic dissipation. Most recently, Saleh et al. [23] analyzed convective heat and mass transfer characteristics of an incompressible MHD visco-elastic fluid flow immersed in a porous medium over a stretching sheet with chemical reaction and thermal stratification.

In another article, Al-Rashdan et al. [2] presented an analytical investigation to the problem of fully developed natural convective heat and mass transfer through porous medium in a vertical channel in the presence of a first order chemical reaction. El-Sayed [7] has presented the theoretical study of the effect of mass diffusion of chemical species with first order reaction on peristaltic motion of an incompressible Jeffery fluid. Additionally, the effect of chemical reaction on the forced and free convection boundary layer that flows in a semi-infinite expanse of an electrically conducting viscous incompressible fluid past a vertical porous plate is carried out by Rajeshwari et al. [22].

Analysis of transport processes and their interaction with chemical reaction has the greatest contributions to many chemical sciences. The chemical reaction effect on heat and mass transfer flow along a semi-infinite horizontal plate has been investigated by Anjalidevi and Kandasamy [3]. Additionally, Patil and Ali [21] analyzed heat and mass transfer from mixed convection flow of polar fluid along a plate in porous media with chemical reaction. A detailed numerical study has been carried out for unsteady hydromagnetic natural convection heat and mass transfer with chemical reaction over a vertical plate in rotating system with periodic suction by Parida et al. [20]. Mahdy [15] have considered effect of chemical reaction and heat generation or absorption on double diffusive convection from vertical truncated cone in a porous media with variable viscosity. Recently, a numerical investigation on the effects of chemical reaction, radiation and magnetic field on the unsteady free convection flow, heat and mass transfer characteristics in a viscous, incompressible and electrically conducting fluid past an exponentially accelerated vertical plate is carried out by Kishore et al. [12]. Most recently, Karunakar et al. [10] investigated effects of heat and mass transfer on MHD mixed convection flow of a vertical surface with radiation, heat source/absorption and chemical reaction. They obtained the results using perturbation method.

This work is an extension of Muthucumaraswamy and Manivannan [18] which studied unsteady free convective flow of a viscous incompressible flow past an infinite isothermal vertical oscillating plate with variable mass diffusion taking into account the homogeneous chemical reaction of first order. The mathematical formulations have taken into cognizance magnetic field, permeability in the momentum equation, variable thermal conductivity and radiation in the energy equation which are absent in Muthucumaraswamy and Manivannan [18]. Also, the boundary conditions for the flow are different.

Hence, in this present study, special attention is given to convective heat and mass transfer flow over a vertical plate with nth order chemical reaction in a porous medium.

2. Mathematical formulation

Consider a free convection unsteady flow of an incompressible, viscous, electrically conducting and chemical reacting fluid with radiative heat and thermal conductivity past a vertical plate through a porous medium. The x' - axis is taken to be along the plate and the y' - axis is taken normal to the plate. A transverse magnetic field of strength B_0 is applied normal to the y-axis. It is assumed that the induced magnetic field, the external electric field and the electric field are negligible. This assumption is justified by the fact that the magnetic Reynolds number is very small. The fluid properties are assumed to be constant. It is also assumed that there exists a homogeneous chemical reaction between the fluid and species concentration. The concentration of diffusing species is very small in comparison to other chemical species, the concentration of species from the wall, C_0' is infinitely small and hence the Soret and Dufour effects are neglected Sarada and Shankar [24].

Under these assumptions and along with Boussinesq's approximation, the governing equation describing the conservation of mass, momentum, energy and concentration are described by the following system of equations respectively:

$$\frac{\partial v'}{\partial y'} = 0 \tag{1}$$

$$\frac{\partial u'}{\partial t'} - v_0 \frac{\partial u'}{\partial y'} = \nu \frac{\partial^2 u'}{\partial y'^2} - \left(\frac{\sigma B_0^{\,2}}{\rho} + \frac{\nu}{k^*} \right) u' + g\beta(T' - T_0') + g\beta^* \left(C' - C_0' \right) \tag{2}$$

International Journal of Scientific Engineering and Technology (ISSN : 2277-1581)
Volume No.3 Issue No.2, pp : 172 – 185 1 Feb 2014

$$\frac{\partial C'}{\partial t'} - v_0 \frac{\partial C'}{\partial y'} = D\frac{\partial^2 C'}{\partial y'^2} - R^*(C' - C_0')^n \qquad (3)$$

$$\frac{\partial T'}{\partial t'} - v_0 \frac{\partial T'}{\partial y'} = \frac{k_0}{\rho C_p}\frac{\partial}{\partial y'}\left[1+\alpha(T'_w - T'_0)\frac{\partial T'}{\partial y'}\right] - \frac{1}{\rho C_p}\frac{\partial q_r}{\partial y'} \qquad (4)$$

The corresponding initial and boundary conditions are prescribed as follows:

$$t \le 0,\ u' = 0,\ T' \to T'_w,\ C' \to C'_w \text{ for all } y'$$

$$t > 0,\ u' = 0,\ T' = T'_w,\ C' = C'_w \text{ at } y' = 0 \qquad (5)$$

$$u' = 0,\ T' = T_0,\ C' = C_0 \quad \text{at } y' = h$$

From continuity equation, it is clear that the suction velocity is either a constant or a function of time. Hence, on integrating equation (1), the suction velocity normal to the plate is assumed in the form,

$$v' = -v_0$$

where v_0 is a scale of suction velocity which is non-zero positive constant. The negative sign indicates that the suction is towards the plate and $v_0 > 0$ corresponds to steady suction velocity normal at the surface. The third and fourth terms on the right hand side of equation (2) denote the thermal and concentration buoyancy effects respectively, The last term of equation (3) is the chemical reaction term and n is the order of chemical reaction which relates the rate of chemical reaction with the concentrations of the reacting substances and the higher the order of the reaction the smaller is the region in the parameters for which multiplicity can occur, while the last term of equation (4) represents the radiative heat flux term.

The Radiative heat flux q_r under Rosseland approximation by Brewster [4] has the form:

$$q_r = -\frac{4\sigma_0'}{3k'}\frac{\partial T'^4}{\partial y'} \qquad (6)$$

where σ_0' is Stefan- Boltzmann constant and k' is the mean absorption coefficient.

We assume that the temperature differences within the flow are so small that T'^4 can be expressed as a linear function of the temperature. This is accomplished by expanding T'^4 in a Taylor series about T_0' and neglecting the higher order terms. Thus

$$T'^4 \cong 4T_0'^3 T' - 3T_0'^4 \qquad (7)$$

Using equations (6) and (7) in equation (4) we obtain:

$$\frac{\partial T'}{\partial t'} - v_0 \frac{\partial T'}{\partial y'} = \frac{k_0}{\rho C_p}\frac{\partial}{\partial y'}\left[1+\alpha(T'_w - T'_0)\frac{\partial T'}{\partial y'}\right] + \frac{16\sigma T_0'^3}{3k'\rho C_p}\frac{\partial^2 T'}{\partial y'^2} \qquad (8)$$

where u' and v' are the Darcian velocity components in the x- and y- directions respectively, t is the time, ν is the kinematic viscosity, g is the acceleration due to gravity, β is the coefficient of volume expansion, ρ the density of the fluid, σ is the scalar electrical conductivity, β^* is the volumetric coefficient of expansion with concentration, C_p is the specific heat capacity at constant pressure, k^* is the permeability of the porous medium, k_0 is the dimensionless thermal conductivity of the ambient fluid, α is a constant depending on the nature of the fluid, $R^*$is the dimensionless chemical reaction, n is the order of chemical reaction, D is the coefficient of molecular diffusivity, v_0 is the constant suction parameter, q_r is the radiative heat flux in the y- direction, B_0 is the magnetic induction of constant strength. T' and T_0' are the temperature of the fluid inside the thermal boundary layer and the fluid temperature in the free stream respectively, while C' and C_0' are the corresponding concentrations.

To obtain the solutions of equations (2), (3) and (8) subject to the conditions (5) in non-dimensional forms, we introduce the following non-dimensional quantities:

$$u=\frac{u'}{u_0},t=\frac{t'u_0}{v},y=\frac{u_0y'}{v},q=\frac{T'-T_0'}{T_w'-T_0'},$$
$$C=\frac{C'-C_0'}{C_w'-C_0'},\Pr=\frac{nrC_p}{u},Sc=\frac{n}{D},$$
$$k=\frac{k^*u_0^2}{v^2},M=\frac{sB_0^2n}{ru_0^2},Gr=\frac{ngb\left(T_w'-T_0'\right)}{u_0^3},\qquad(9)$$
$$Gc=\frac{ngb^*\left(C_w'-C_0'\right)}{u_0^3},l=a\left(T_w'-T_0'\right),$$
$$g=\frac{n_0}{u_0},K_r=\frac{R^*n}{u_0^2},R=\frac{16as_0'nT_0'^3}{k'u_0^2}$$

Applying these non-dimensionless quantities (9), the set of equations (2), (3), (8), and (5) reduces to the following:

$$\frac{\partial u}{\partial t}-\gamma\frac{\partial u}{\partial y}=\frac{\partial^2u}{\partial y^2}-\left(M+\frac{1}{k}\right)u+Gr\theta+GcC\qquad(10)$$

$$\frac{\partial C}{\partial t}-\gamma\frac{\partial C}{\partial y}=\frac{1}{Sc}\frac{\partial^2C}{\partial y^2}-K_rC^n\qquad(11)$$

$$\frac{\partial\theta}{\partial t}-\gamma\frac{\partial\theta}{\partial y}=\frac{\lambda}{\Pr}\left(\frac{\partial\theta}{\partial y}\right)^2+\frac{1}{\Pr}(1+\lambda\theta)\frac{\partial^2\theta}{\partial y^2}-\frac{R}{\Pr}\theta\qquad(12)$$

With the following initial and boundary conditions

$$\begin{aligned}&t\le0\ u=0,\ \theta=0,\ C=0,\ for\ all\ y,\\&t>0\ u=0,\ \theta=1,\ C=1,\ at\ y=0,\\&\quad u=0,\ \theta=0,\ C=0\ at\ y=1.\end{aligned}\qquad(13)$$

where $\Pr$ is the Prandtl number, Sc is the Schmidt number, M is the Magnetic field parameter, Gr is the thermal Grashof number, Gc is the solutal or mass Grashof number, λ is the variable thermal conductivity, γ is the variable suction parameter, R is the radiation parameter, K_r is the chemical reaction parameter, n is the order of chemical reaction, k is the permeability parameter, t is the dimensionless time while u and v are dimensionless velocity components in x- and y-directions respectively.

3. Analytical solutions

The governing equations involved in this problem are highly coupled and non linear. In order to confirm the validity of this model, it is therefore of interest to reduce the governing equations of this problem to a form that can be solved analytically. A special case of this problem that exhibits approximate solution is the problem of steady convective heat and mass transfer flow over a vertical plate with chemical reaction and porous media. The steady state equations and boundary conditions for the problem can be written as follows:

$$\frac{\partial^2u}{\partial y^2}+\gamma\frac{\partial u}{\partial y}-\left(M+\frac{1}{k}\right)u+Gr\theta+GcC=0\qquad(14)$$

$$\frac{\partial^2C}{\partial y^2}+\gamma Sc\frac{\partial C}{\partial y}-K_rScC=0\qquad(15)$$

$$\frac{\partial^2\theta}{\partial y^2}+\gamma\Pr\frac{\partial\theta}{\partial y}-R\theta=0\qquad(16)$$

The boundary conditions are:

$$\begin{aligned}&u=0,\ \theta=1,\ C=1,\quad at\ y=0,\\&u=0,\ \theta=0,\ C=0\quad at\ y=1.\end{aligned}\qquad(17)$$

To find the approximate solution to equations (14)-(16) subject to equation (17), we use perturbation method which is a method that is used to approximate the solution to a differential equation analytically. Therefore the physical variables u, C, and θ can be expanded in the power of $(R<<1)$. This can be possible physically as R for the flow is always less than unity. Hence we can assume solution of the form

$$\begin{aligned}u&=u_0(y)+Ru_1(y)+0(R^2)\\C&=C_0(y)+RC_1(y)+0(R^2)\\\theta&=\theta_0(y)+R\theta_1(y)+0(R^2)\end{aligned}\qquad(18)$$

Using equation (18) in equations (14)-(17) and equating the coefficient of like powers of R, we have

$$u_0'' + \gamma u_0' - \left(M + \frac{1}{k}\right)u_0 = -Gr\theta_0 - GcC_0 \quad (19)$$

$$C_0'' + \gamma ScC_0' - K_r ScC_0 = 0 \quad (20)$$

$$\theta_0'' + \gamma \Pr \theta_0' = 0 \quad (21)$$

$$u_1'' + \gamma u_1' - \left(M + \frac{1}{k}\right)u_1 = -Gr\theta_1 - GcC_1 \quad (22)$$

$$C_1'' + \gamma ScC_1' - K_r ScC_1 = 0 \quad (23)$$

$$\theta_1'' + \gamma \Pr \theta_1' = \theta_0 \quad (24)$$

The corresponding boundary conditions are

$$\begin{aligned} &u_0 = 0, \quad \theta_0 = 1, \quad C_0 = 1 \\ &u_1 = 0, \quad \theta_1 = 0, \quad C_1 = 0 \qquad at \quad y = 0 \\ &u_0 = 0, \quad \theta_0 = 0, \quad C_0 = 0 \\ &u_1 = 0, \quad \theta_1 = 0, \quad C_1 = 0 \qquad at \quad y = 1 \end{aligned} \quad (25)$$

Solving equations (19)-(24) with the help of equation (25), we get

$$u_0 = L_9 e^{s_1 y} + L_{10} e^{s_2 y} + L_{11} + L_{12} e^{-\gamma \Pr y} + L_{13} e^{h_1 y} + L_{14} e^{h_2 y} \quad (26)$$

$$u_1 = L_{15} e^{s_1 y} + L_{16} e^{s_2 y} + L_{17} + L_{18} e^{-\gamma \Pr y} + \left(L_{19} y + L_{20}\right) e^{-\gamma \Pr y} \quad (27)$$

$$C_0 = L_7 e^{h_1 y} + L_8 e^{h_2 y} \quad (28)$$

$$C_1 = 0 \quad (29)$$

$$\theta_0 = L_1 + L_2 e^{-\gamma \Pr y} \quad (30)$$

$$\theta_1 = L_3 + L_4 e^{-\gamma \Pr y} + \left(L_5 - L_6\right) y e^{-\gamma \Pr y} \quad (31)$$

In view of the above equations the solutions are

$$u = L_9 e^{s_1 y} + L_{10} e^{s_2 y} + L_{11} + L_{12} e^{-\gamma \Pr y} + L_{13} e^{h_1 y} + L_{14} e^{h_2 y} + R\begin{bmatrix} L_{15} e^{s_1 y} + L_{16} e^{s_2 y} + L_{17} + L_{18} e^{-\gamma \Pr y} \\ + \left(L_{19} y + L_{20}\right) e^{-\gamma \Pr y} \end{bmatrix} \quad (32)$$

$$C = L_7 e^{h_1 y} + L_8 e^{h_2 y} \quad (33)$$

$$\theta = L_1 + L_2 e^{-\gamma \Pr y} + R\begin{bmatrix} L_3 + L_4 e^{-\gamma \Pr y} + \\ \left(L_5 - L_6\right) y e^{-\gamma \Pr y} \end{bmatrix} \quad (34)$$

4. Numerical solutions

The system of transformed coupled non-linear partial differential equations (10), (11) and (12) together with the initial and boundary conditions (13) have been solved numerically using a finite difference technique of implicit type namely Crank-Nicolson implicit finite difference method which is always convergent and stable. The equivalent finite difference approximations corresponding to equations (10)-(12) are given as follows:

$$\left(\frac{u_{i,j+1} - u_{i,j}}{\Delta t}\right) - \frac{\gamma}{2\Delta y}\left(u_{i+1,j} - u_{i-1,j}\right) = \frac{1}{2\left(\Delta y^2\right)}\left(\begin{matrix} u_{i+1,j+1} - 2u_{i,j+1} + u_{i-1,j+1} + \\ u_{i+1,j} - 2u_{i,j} + u_{i-1,j} \end{matrix}\right) - \left(M + \frac{1}{k}\right)u_{i,j} + Gr\left(\theta_{i,j}\right) + Gc\left(C_{i,j}\right) \quad (35)$$

$$\left(\frac{C_{i,j+1} - C_{i,j}}{\Delta t}\right) - \frac{\gamma}{2\Delta y}\left(C_{i+1,j} - C_{i-1,j}\right) = \frac{1}{2Sc\left(\Delta y^2\right)}\left(\begin{matrix} C_{i+1,j+1} - 2C_{i,j+1} + \\ C_{i-1,j+1} + C_{i+1,j} - 2C_{i,j} + C_{i-1,j} \end{matrix}\right) - K_r\left(C_{i,j}\right)^n \quad (36)$$

$$\left(\frac{\theta_{i,j+1}-\theta_{i,j}}{\Delta t}\right)-\frac{\gamma}{2\Delta y}\left(\theta_{i+1,j}-\theta_{i-1,j}\right)=$$
$$\frac{H}{2\,\mathrm{Pr}\left(\Delta y^2\right)}\begin{pmatrix}\theta_{i+1,j+1}-2\theta_{i,j+1}+\theta_{i-1,j+1}+\\ \theta_{i+1,j}-2\theta_{i,j}+\theta_{i-1,j}\end{pmatrix}+ \qquad (37)$$
$$\frac{\lambda}{\mathrm{Pr}\left(\Delta y^2\right)}\left(\theta_{i+1,j}-\theta_{i,j}\right)^2-\frac{R}{\mathrm{Pr}}\left(\theta_{i,j}\right)$$

The initial and boundary conditions take the following forms:

$$\begin{aligned} &u_{i,j}=0, \quad \theta_{i,j}=0, \quad C_{i,j}=o \\ &u_{0,j}=0, \quad \theta_{0,j}=1, \quad C_{0,j}=1 \\ &u_{h,j}=0, \quad \theta_{h,j}=0, \quad C_{h,j}=o \end{aligned} \qquad (38)$$

where h corresponds to 1.

The index *i* refers to space *y* and *j* refers to time *t*. Δy and Δt are the mesh sizes along *y* - direction and time *t* - direction respectively. The Finite difference equations (35)-(37) at every internal nodal point on a particular n-level constitute a tri-diagonal system of equations which are solved by using the Thomas Algorithm.

In each time step, the concentration and temperature profiles have been computed first from equations (36) and (37) and then the computed values are used to obtain the velocity profile at the end of time steps that is $u_{i,j+1}$ computed from equation (34). This process is carried out until the steady state solution of the convergence criteria for stability of the scheme is assumed to have been reached. Computations are carried out for different values of physical parameters involved in the problem.

The skin friction coefficient, the Nusselt number and Sherwood number at the plate are given by:

$$C_f=\left(\frac{\partial u}{\partial y}\right)_{y=0}, Nu=-\left(\frac{\partial \theta}{\partial y}\right)_{y=0}, Sh=\left(\frac{\partial C}{\partial y}\right)_{y=0} \qquad (39)$$

5. Results and discussion

In order to get a physical view of the present problem, numerical computations have been carried out for different values of thermal Grashof number (Gr), solutal Grashof number (Gc), Magnetic parameter (M), porous parameter (k), suction parameter (γ), radiation parameter (R), chemical reaction parameter (K_r), order of chemical reaction (n), variable thermal conductivity (λ), Prandtl number (Pr) and Schmidt number (Sc). The purpose of this computation given here is to assess the effect of these physical parameters upon the nature of the flow and transport. Computations are obtained for fluids with Prandtl number (Pr = 0.71, 1.0 and 7.0) corresponding to air, salt water and water respectively. The diffusing chemical species of most common interest in air have Schmidt number and is taken for (*Sc* = 0.22 0.60) which corresponds to hydrogen and oxygen respectively. The default values of the physical parameters are as follows:

$$Gr=2.0, Gc=2.0, M=1.0, K_r=2.0, \mathrm{Pr}=0.71,$$
$$Sc=0.22, R=1.0, k=0.1, n=0.1, \gamma=0.2, \lambda=1.0.$$

All graphs therefore correspond to these values unless specifically indicated on the appropriate graphs.

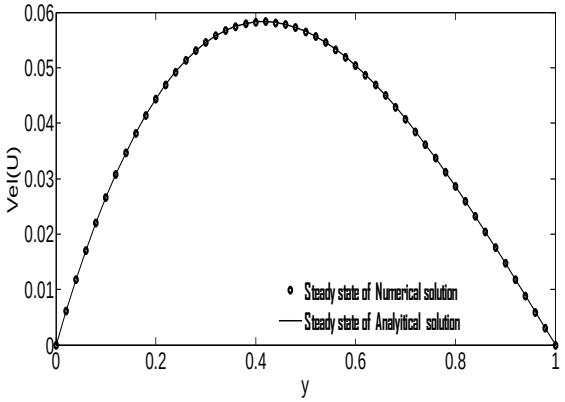

Fig. 1. Steady- state solution of Velocity profile for numerical and analytical solutions.

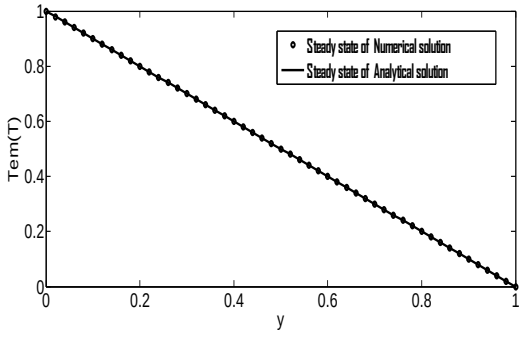

International Journal of Scientific Engineering and Technology (ISSN : 2277-1581)
Volume No.3 Issue No.2, pp : 172 – 185 1 Feb 2014

Fig. 2. Steady-state solution of Temperature profile for numerical and analytical solutions.

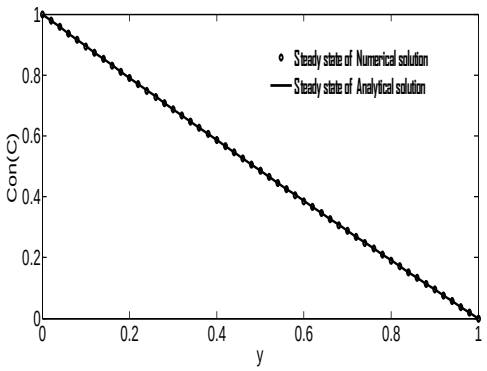

Fig. 3. Steady-state solution of Concentration profile for numerical and analytical solutions.

Figures (1)-(3) present comparison of the steady-state solution for numerical and analytical solutions of velocity, temperature and concentration profiles respectively.These results are presented to illustrate the accuracy of the numerical and analytical solutions. It is observed that the time necessary to reach the steady-state solution is $t_{\max}$,where $t_{\max}$ is the steady-state value of time (t). Hence, the numerical solution for the problem is in good agreement with analytical solution at time $t_{\max}$.

Figures (4) to (22) are all plotted at time $t = 0.2$ respectively.

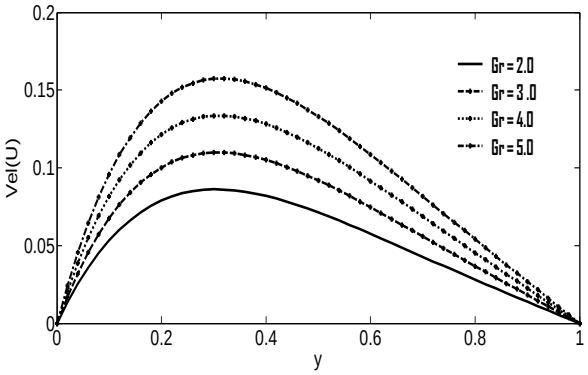

Fig. 4. Velocity profile for different values of thermal Grashof number (Gr).

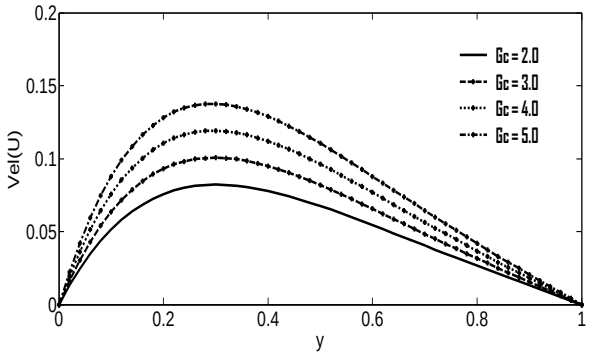

Fig. 5. Velocity profile for different values of solutal Grashof number (Gc).

Figures (4) and (5) describe typical velocity profiles in the boundary layer for various values of thermal Grashof number and solutal Grashof number in cases of cooling of the surface respectively. It is observed that an increase in Gr and Gc results in an increasing momentum boundary layer, this is due to the fact that increasing the values of Gr and Gc has the tendency to increase the thermal and mass buoyancy effect. This gives a rise to an increase in the induced flow.

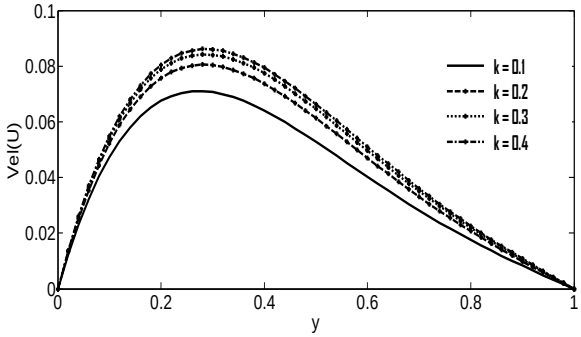

Fig. 6. Velocity profile for different values of porosity parameter (k)

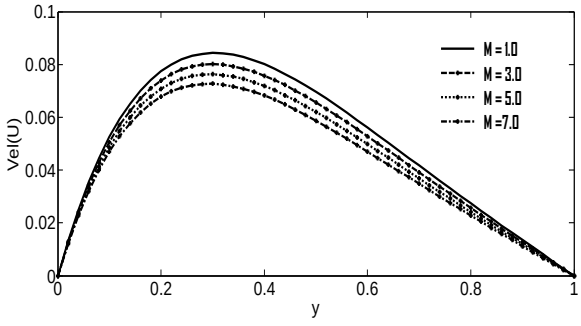

Fig. 7. Velocity profile for different values of Magnetic parameter (M).

Figure (6) depicts the variation of velocity distribution across the boundary layer for various values of porous parameter k . The porosity medium has considerably effect on the velocity. An increase in porosity leads to increasing velocity profiles. The effect of magnetic parameter M on the velocity profile in the boundary layer is displayed in figure (7). Application of a transverse magnetic field produces a resistive-type force called the Lorentz force. This force has the tendency to slow down the motion of the fluid in the momentum boundary layer.

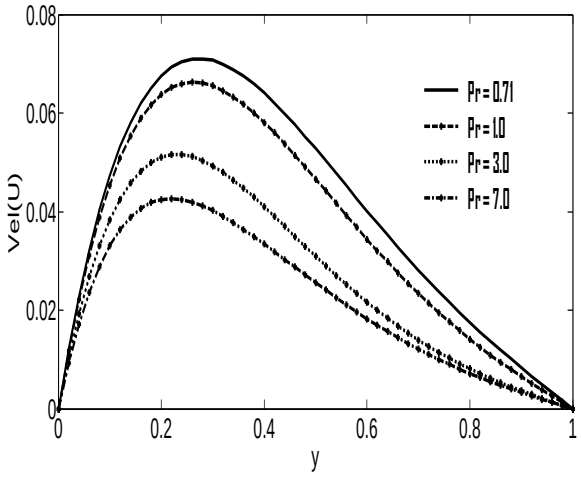

Fig. 8. Velocity profile for different values of Prandtl number (Pr)

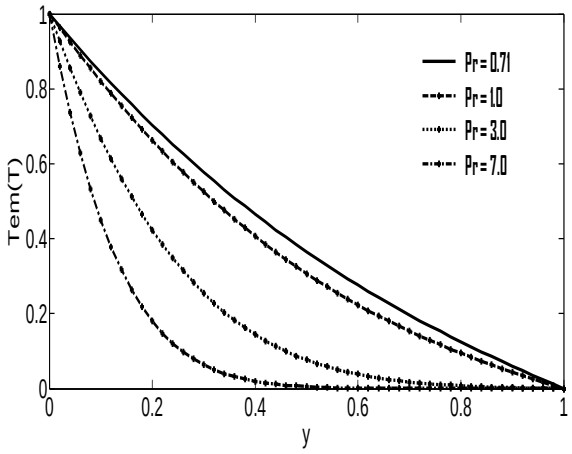

Fig. 9. Temperature profile for different values of Prandtl number (Pr)

Figures (8) and (9) describe the behavior of Prandtl number on velocity profile and temperature distribution. It is seen that momentum and thermal boundary layer both decrease with the increase in Prandtl number. This is because smaller values of Pr are equivalent to increasing the thermal conductivities and therefore heat is able to diffuse away from the heated plate more rapidly than for higher values of Pr .

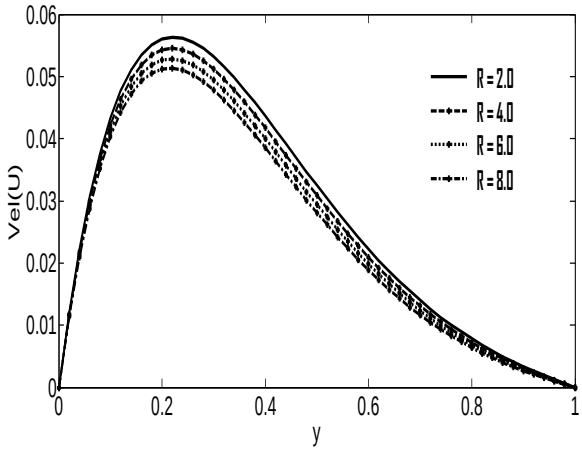

Fig. 10. Velocity profile for different values of Radiation parameter (R)

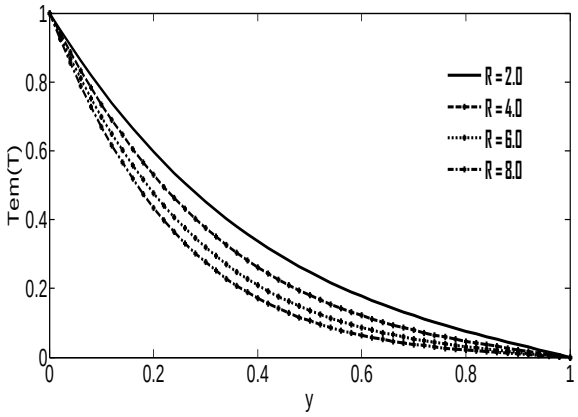

Fig. 11. Temperature profile for different values of Radiation parameter (R)

The effect of radiation parameter R on the velocity and temperature profiles are plotted in figures (10) and (11). It is observed that as the value of radiation parameter increases the velocity and temperature profiles decreases with a decreasing in the momentum and thermal boundary layer thickness.

International Journal of Scientific Engineering and Technology (ISSN : 2277-1581)
Volume No.3 Issue No.2, pp : 172 – 185 1 Feb 2014

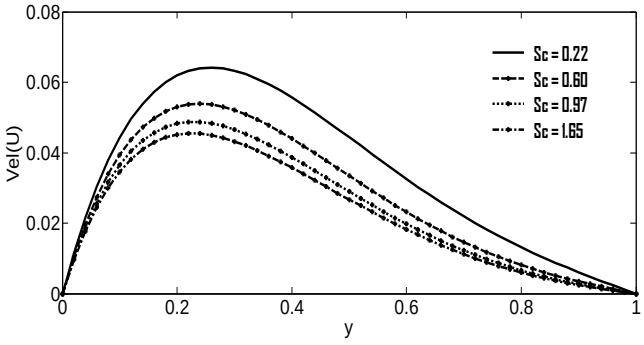

Fig. 12. Velocity profile for different values of Schmidt number (*Sc*)

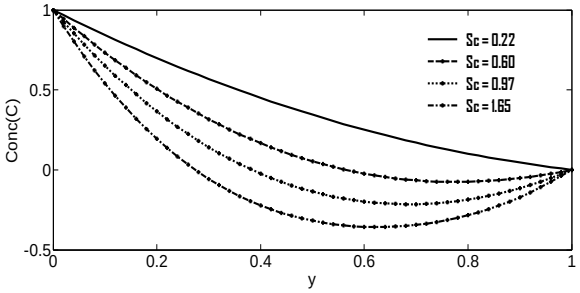

Fig. 13. Concentration profile for different values of Schmidt number (*Sc*)

In figures (12) and (13) the influence of Schmidt number *Sc* on velocity and concentration are displayed respectively. As the Schmidt number increases, the velocity and concentration decreases. This causes the concentration buoyancy effect to decrease yielding a reduction in the fluid velocity and concentration. Physically, increase of *Sc* means decrease in molecular diffusivity.

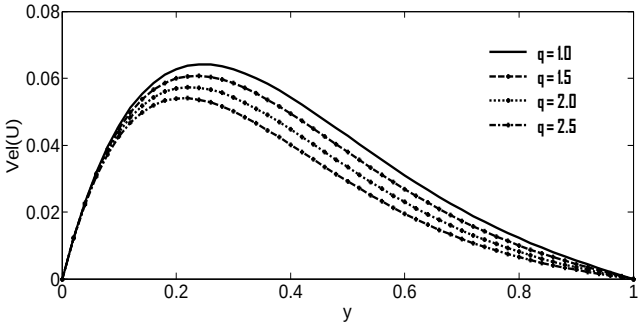

Fig. 14. Velocity profile for different values of Suction parameter (γ = q)

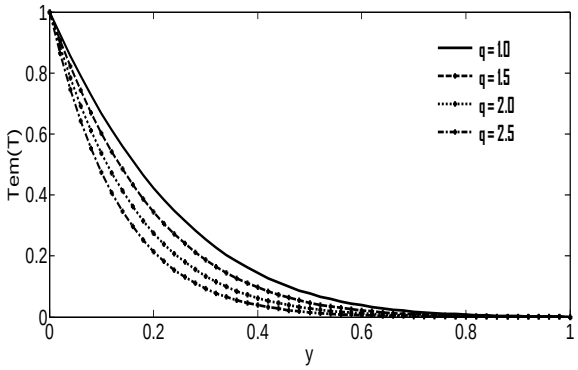

Fig. 15. Temperature profile for different values of Suction parameter (γ = q)

Figures (14) and (15) represent respectively the velocity and temperature profiles for various values of suction parameter. It is noticed that the velocity and temperature profiles decreases monotonically with increasing suction parameter which indicating the usual fact that suction parameter stabilizes the boundary layer growth.

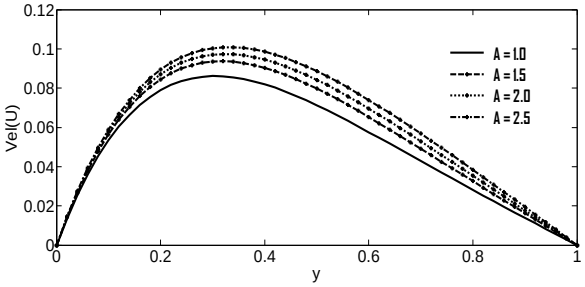

Fig. 16. Velocity profile for different values of Thermal conductivity (λ = A)

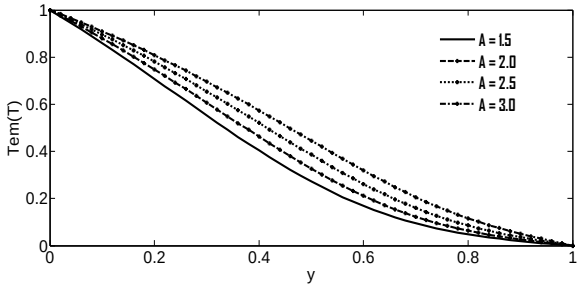

Fig. 17. Temperature profile for different values of Thermal conductivity (λ = A)

Figures (16) and (17) illustrate the effect of thermal conductivity parameter on the velocity distribution and temperature profile respectively. Increase in the mixed convection parameter leads to increasing in the fluid flow and thermal boundary layer respectively.

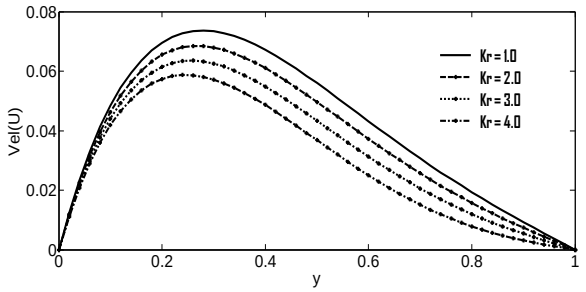

Fig. 18. Velocity profile for different values of Chemical reaction parameter (K_r)

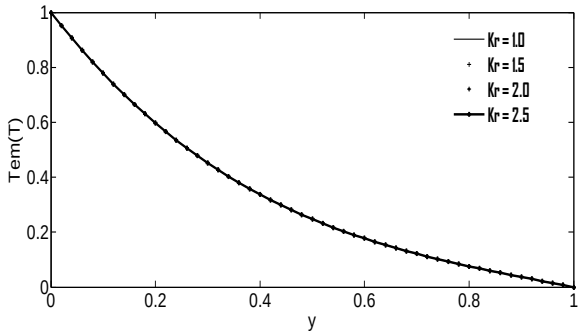

Fig. 19. Temperature profile for different values of Chemical reaction parameter (K_r)

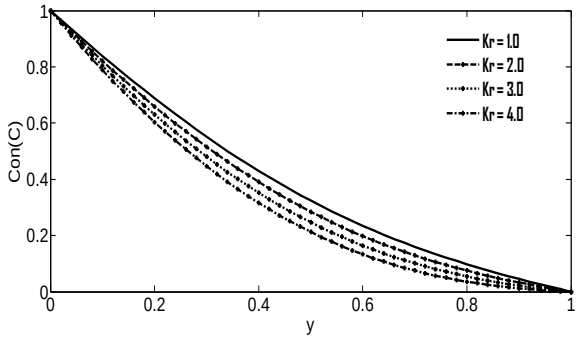

Fig. 20. Concentration profile for different values of Chemical reaction parameter (K_r)

Figures (18)-(20) depicts the influence of chemical reaction parameter on the velocity, temperature and concentration profiles in the boundary layer respectively. As shown the velocity and concentration are decreasing with increasing K_r, but the temperature profile increases as K_r increases, this is due to the fact that destructive chemical reduces the solutal boundary layer thickness.

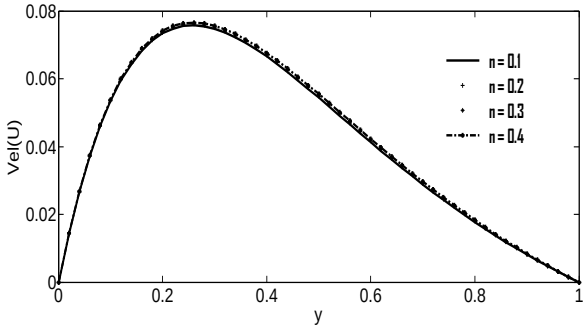

Fig. 21.Velocity profile for different values of order Chemical reaction (n)

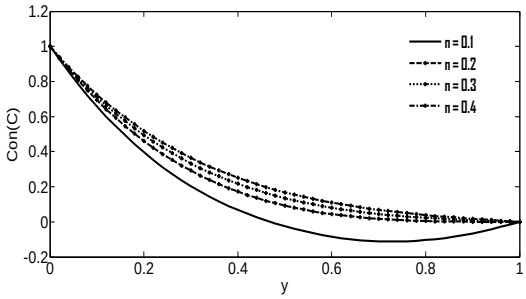

Fig. 22. Concentration profile for different values of order Chemical reaction (n)

The effects of order chemical reaction (n) on the velocity and concentration profiles are displayed in figures (21) and (22) respectively. It is observed from these figures that an increase in the chemical reaction order increases the velocity and concentration profiles respectively.

International Journal of Scientific Engineering and Technology (ISSN : 2277-1581)
Volume No.3 Issue No.2, pp : 172 – 185 1 Feb 2014

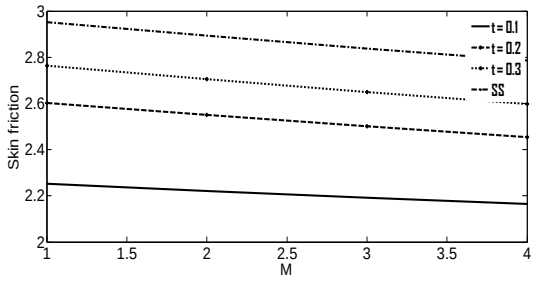

Fig. 23. Skin friction for different values of *t* for Pr = 0.71

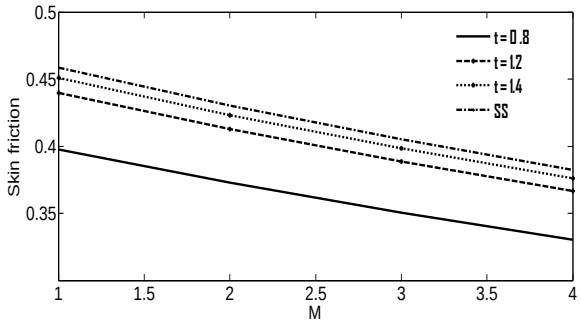

Fig. 24. Skin friction for different values of *t* for Pr =7.0

In figures (23) and (24), skin friction is plotted against magnetic parameter M for different values of non-dimensional time (t) and Prandtl number ($\Pr = 0.71, 7.0$). It is observed that as magnetic parameter and time increases the steady-state of the skin friction increases for both air ($\Pr = 0.71$) and water ($\Pr = 7.0$) respectively.

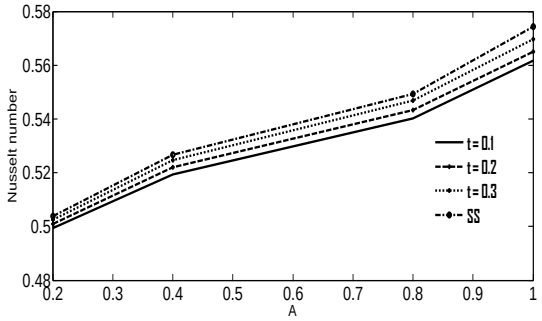

Fig. 25. Nusselt number for different values of *t* for Pr =0.71

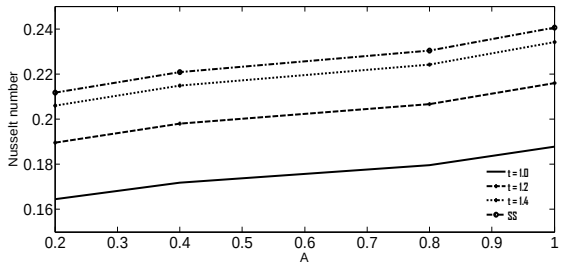

Fig. 26. Nusselt number for different values of *t* for Pr =7.0

Figures (25) and (26) show representative profiles for Nusselt number (rate of heat transfer) for different values of non-dimensional time (t) and thermal conductivity (λ = A) for Prandtl number ($\Pr = 0.71, 7.0$). These figures reflects that an increase in time t and λ increases the rate of heat transfer, this is physically true because as λ increases the fluid temperature increases and consequently there is high rate of heat transfer on the boundary.

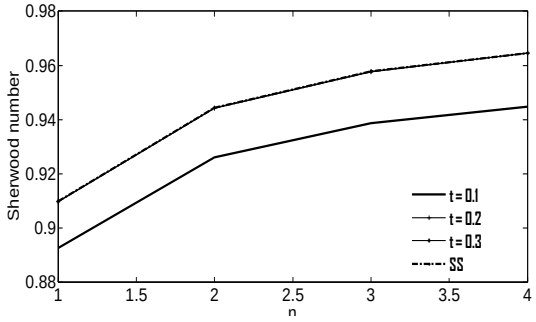

Fig. 27. Sherwood number for different values of *t* for *Sc* = 0.22

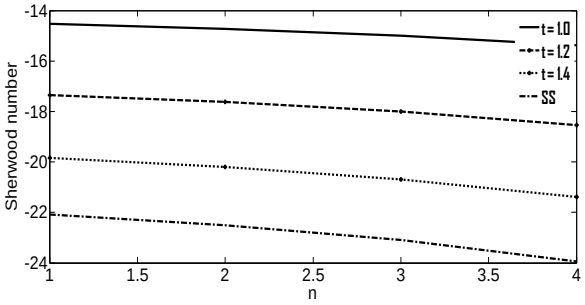

Fig. 28. Sherwood number for different values of *t* for *Sc* = 0.60.

Figures (27) and (28) describe the behavior of Sherwood number against order of chemical reaction (n) with different values of time t for Schmidt number ($Sc = 0.22, 0.60$). It is observed that as n and t increases the Sherwood number increases for hydrogen ($Sc = 0.22$) and decreases for water vapor ($Sc = 0.60$).

6. Conclusion

The present numerical study has been carried out for convective heat and mass transfer flow over a vertical plate with nth order chemical reaction in a porous medium. An implicit finite difference method of Crank-Nicolson is employed to solve the equations governing the flow. The following conclusion has been drawn for the present numerical investigation.

1. It is found out that the velocity profiles increases with increasing thermal Grashof number, solutal Grashof number, porous material, order of chemical reaction and thermal conductivity. It is also interesting to note that increase in magnetic parameter, chemical reaction, Prandtl number, radiation, Schmidt number and suction leads to decreasing the flow velocity.

2. An increasing Prandtl number, radiation parameter, chemical reaction and suction decreases the temperature profiles of the fluid flow field at all points. However, the temperature increases with increasing thermal conductivity and chemical reaction.

3. The concentration profile increases with increasing value in order of chemical reaction whereas it decreases with the increasing values of Schmidt number and chemical reaction.

4. Skin friction increases with increasing magnetic field and time t.

5. The rate of heat transfer in terms of Nusselt number increases with increasing thermal conductivity and time.

6. An increasing order of chemical reaction increases Sherwood number for hydrogen (*Sc* = 0.22) and decreases for water vapor (*Sc* = 0.60).

7. The numerical solution is in excellent agreement with the analytical solution at time $t_{\max}$.

Acknowledgment

The author Halima Usman is thankful to Usmanu Danfodiyo University, Sokoto for financial support.

Appendix

$$h_1 = \frac{-\gamma + \sqrt{\gamma^2 Sc^2 + 4K_r Sc}}{2}, h_2 = \frac{-\gamma - \sqrt{\gamma^2 Sc^2 + 4K_r Sc}}{2},$$

$$s_1 = \frac{-\gamma + \sqrt{\gamma^2 + 4r_4}}{2}, s_2 = \frac{-\gamma - \sqrt{\gamma^2 + 4r_4}}{2},$$

$$L_1 = 1 - L_2, L_2 = \frac{-1}{e^{-\gamma \Pr} - 1}, L_3 = -L_4,$$

$$L_4 = \frac{L_2 e^{-\gamma \Pr}}{\gamma \Pr\left(e^{-\gamma \Pr} - 1\right)} - \frac{L_1 e^{-\gamma \Pr}}{\gamma \Pr\left(e^{-\gamma \Pr} - 1\right)},$$

$$L_5 = \frac{L_1}{\gamma \Pr}, L_6 = \frac{L_2}{\gamma \Pr}, L_7 = 1 - L_8, L_8 = \frac{-e^{h_1}}{e^{h_2} - e^{h_1}},$$

$$L_9 = -\left(L_{10} + L_{11} + L_{12} + L_{13} + L_{14}\right), L_{10} = \frac{L_{11}\left(e^{s_1} - 1\right)}{e^{s_2} - e^{s_1}} +$$

$$\frac{L_{12}\left(e^{s_1} - e^{-\gamma \Pr}\right)}{e^{s_2} - e^{s_1}} + \frac{L_{13}\left(e^{s_1} - e^{h_1}\right)}{e^{s_2} - e^{s_1}} + \frac{L_{14}\left(e^{s_1} - e^{h_2}\right)}{e^{s_2} - e^{s_1}},$$

$$L_{11} = \frac{GrL_1}{r_4}, L_{12} = -\frac{GrL_2}{\gamma^2 \Pr^2 - \gamma^2 \Pr - r_4}, L_{13} = -\frac{GcL_7}{h_1^2 + \gamma h_1 - r_4},$$

$$L_{14} = -\frac{GcL_8}{h_2^2 + \gamma h_2 - r_4}, L_{15} = -\left(L_{16} + L_{17} + L_{18} + L_{20}\right),$$

$$L_{16} = \frac{-L_{17}\left(1 - e^{s_1}\right)}{e^{s_2} - e^{s_1}} - \frac{L_{18}\left(e^{-\gamma \Pr} - e^{s_1}\right)}{e^{s_2} - e^{s_1}} -$$

$$\frac{L_{19}\left(e^{-\gamma \Pr} - e^{s_1}\right)}{e^{s_2} - e^{s_1}} - \frac{L_{20}\left(e^{-\gamma \Pr} - e^{s_1}\right)}{e^{s_2} - e^{s_1}}, L_{17} = \frac{GrL_3}{r_4},$$

$$L_{18} = -\frac{GrL_4}{\gamma^2 \Pr^2 - \gamma^2 \Pr - r_4}, L_{19} = \frac{E}{\gamma^2 \Pr^2 - \gamma^2 \Pr - r_4},$$

$$L_{20} = \frac{-L_{19}\left(\gamma - 2\gamma \Pr\right)}{\gamma^2 \Pr^2 - \gamma^2 \Pr - r_4}, E = \left(\frac{GrL_2}{\gamma \Pr} - \frac{GrL_1}{\gamma \Pr}\right).$$

Nomenclature

C – Concentration

C_p – Specific heat at constant pressure

D - Mass diffusivity

g – Acceleration due to gravity

Gr – Grashof number
Gc – Solutal Grashof number
k – Porous parameter
Nu – Nusselt number
Pr – Prandtl number
Sc – Schmidt number
R - Radiation parameter
K_r - Chemical reaction parameter
n - order of chemical reaction
T – Temperature
C_f -Skin friction
SS- Steady-State
Sh - Sherwood number
u, v – velocities in the x and y-direction respectively
x, y – Cartesian coordinates along the plate and normal to it respectively
B_0 - Magnetic field of constant strength
M – Magnetic field parameter

Greek Letters

β* - coefficient of expansion with concentration
β - Coefficient of thermal expansion
$\sigma_0^{'}$ - Stefan-Boltzmann constant
σ -Scalar electrical conductivity
ρ- Density of fluid
θ- dimensionless temperature
υ- Kinematic viscosity
γ - Suction parameter
λ - Variable thermal conductivity

Subscripts

w - condition at wall
∞ - condition at infinity

References

i. *N. Ahmad, J.K. Goswami, D.P. Barua. Effects of chemical reaction and radiation on an unsteady MHD flow past an accelerated infinite vertical plate with variable temperature and mass transfer, Indian Journal of Pure and Applied Mathematics, 44(4) (2013) 443-466.*

ii. *M. Al-Rashdan, S.M. Fayyad, M. Farihat. Heat and Mass Fully-Developed natural convective viscous flow with chemical reaction in porous medium, Advanced Theoretical Applied Mechanics, 5(3) (2012) 93-112.*

iii. *S.P. Anjalidevi, R. Kandasamy. Effect of chemical reaction Heat and Mass transfer on laminar flow along a semi-infinite horizontal plate, International Journal of Heat and Mass Transfer, 35(6) (1999) 465-467.*

iv. *M.Q. Brewster. Thermal Radiative Transfer and Properties, John Wiley and Sons. Inc, New York (1992).*

v. *B.C. Chandrasekhara, P.M.S. Namboodiri. International Journal of Heat Mass Transfer, 28 (1985) 199-206.*

vi. *P. Dilal, S. Chatterjee. MHD mixed convective Heat and Mass transfer in a visco-elastic fluid in a porous medium towards a stretching sheet with viscous-ohmic heating and chemical reaction, The Canadian Journal of Chemical Engineering, DOI:10.1002/CJCE.21829 (2013).*

vii. *M.F. El-Sayed, N.T.M. Eldabe, A.Y. Ghaly. Effects of chemical reaction, Heat and Mass transfer on Non-Newtonian fluid flow through porous medium in a vertical peristaltic tube, Transport Porous Medium, 89 (2011) 185-212.*

viii. *C.S. Gregory, A.A. Ilhan. Simultaneous momentum Heat and Mass transfer with chemical reaction in a disordered porous medium: Application to Binder removal from a ceramic green body, Chemical Engineering Science, 45(7) (1988) 1719-1731.*

ix. *S. Gurminder, P.R. Sharma, A.J. Chamkha. Mass transfer with chemical reaction in MHD mixed convective flow along a vertical stretching sheet, International Journal of Energy and Technology, 4(20) (2012) 1-12.*

x. *S. R. Karunakar, D. C. Kesavaiah, M. N. R. Shekar. Convective Heat and Mass transfer flow from a vertical surface with radiation, chemical reaction and heat source/absorption, International Journal of Scientific Engineering and Technology, 2(5) (2013) 351-361.*

xi. *A. M. Kawala, S. N. Odda. Numerical investigation of unsteady free convection on a vertical cylinder with variable Heat and Mass flux in the presence of chemical reactive species, Advances in Pure Mathematics, 3(1A) (2013) 183-189.*

xii. *P. M. Kishore, N. V. Prasada, S. V. Varma, S. Vantarakamana. The effects of radiation and chemical reaction on unsteady MHD free convection flow of viscous fluid past an exponentially accelerated vertical plate, International Journal of Physical and Mathematical Sciences, 4(1) (2013) 300-317.*

xiii. *B. Krishnendu. Slip effects on boundary layer flow and Mass transfer with chemical reaction over a permeable flat plate embedded in*

a Darcy porous medium, Frontiers in Heat and Mass Transfer, 3(4) (2012) 1-6.

xiv. P. T. Loganathan, Kulandaivel, R. Muthucumuraswamy. First order chemical reaction on moving semi-infinite vertical plate in the presence of optically thin gray gas, International Journal of Applied Mathematics and Mechanics, 4(5) (2008) 26-41.

xv. A. Mahdy. Effect of chemical reaction and heat generation /absorption on double-diffusive convection from a vertical truncated cone in a porous media with variable viscosity, International Communications in Heat and Mass Transfer, 37(5) (2010) 548-554.

xvi. M. A. Mansour, N. F. El-Anssary, A. M. Aly. Effect of chemical reaction and viscous dissipation on MHD natural convection flows saturated in porous media with suction or injection, International Journal of Applied Mathematics and Mechanics, 4(2) (2008) 60-70.

xvii. B .J. Minto, D. B. Ingham, I. Pop. Free convection driven by an exothermic reaction on a vertical surface embedded in a porous media, International Journal of Heat and Mass Transfer, 41(1) (1998) 11-23.

xviii. R. Muthucumaraswamy, K. Manivannan, First order chemical reaction on isothermal vertical oscillating plate with variable mass diffusion, International Journal of Pure and Applied Sciences and Technology, 39(1) (2011) 19-26.

xix. D. A. Nield, A. Bejan. Convection in porous media, 2nd edition, Springer-Verlag, New York, (1999).

xx. S. K. Parida, M. Acharya, G. C. Dash, S. Panda. MHD Heat and Mass transfer in a rotating system with periodic suction, Arabian Journal of Science and Engineering, 36(6) (2011) 1139-1151.

xxi. P. M. Patil, A. J. Chamkha. Heat and Mass transfer from mixed convection flow of polar fluid along a plate in porous media with chemical reaction, International Journal of Numerical Methods for Heat and Fluid Flow, 23(5) (2013) 899-926.

xxii. R. Rajeshwari, B. Jothiram, V. K. Nelson. Chemical reaction, Heat and Mass transfer on non linear MHD boundary layer flow through a vertical porous plate in the presence of suction. Applied Mathematical Sciences, 3(50) (2009) 2469-2480.

xxiii. M. A. Saleh, A. A. Mohamed, S. E. Mahmoud. Heat and Mass transfer in MHD visco-elastic fluid flow through a porous medium over a stretching sheet with chemical reaction, Journal of Applied Mathematics, 1 (2010) Doi: 10.4236. 446 - 455.

xxiv. Sarada, Shankar. Chemical reaction effect on an unsteady MHD convective flow past an infinite vertical moving plate embedded in a porous medium with heat source, Journal of Global Research in Mathematical Archives, 1(5) (2013) 63-81.